The Abdus Salam International Centre for Theoretical Physics

United Nations Educational, Scientific and Cultural Organization

IAEA International Atomic Energy Agency

2142-1

Advanced Conference on Seismic Risk Mitigation and Sustainable Development

10 - 14 May 2010

PSHA and NDSHA in Italy

G.F. Panza

University of Trieste/ICTP
Trieste

PSHA and NDSHA in Italy

by

Giuliano F. Panza

Advanced Conference on Seismic Risk Mitigation & Sustainable Development
ICTP 10-14 May, 2010

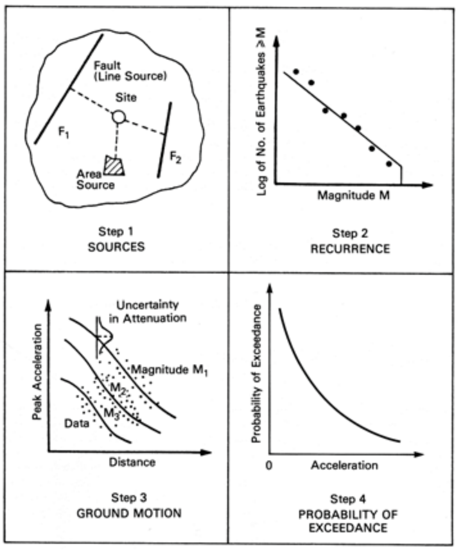

FIGURE 10.2 Basic steps of probabilistic seismic hazard analysis (after TERA Corporation 1978).

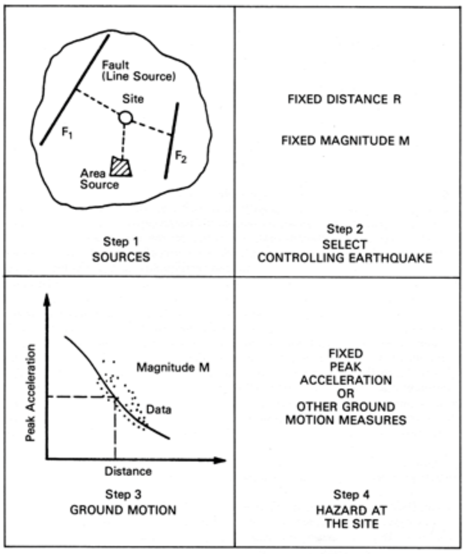

FIGURE 4.1 Basic steps of deterministic seismic hazard analysis (after TERA Corporation 1978).

Probabilistic and Deterministic

procedures after Reiter (1990)

Probabilistic

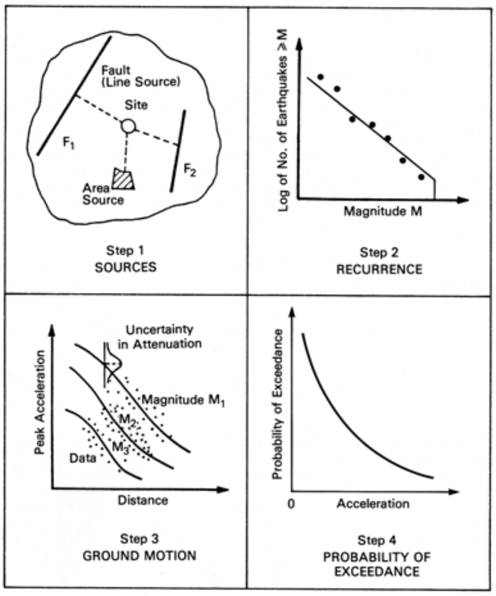

FIGURE 10.2 Basic steps of probabilistic seismic hazard analysis (after TERA Corporation 1978).

Step 2 - Recurrence can be represented by a linear relation only if the size of the study area is large with respect to linear dimensions of sources.

Step 3 - Attenuation relations are usually not translation invariant in the phase space (M, R, S), i.e. the relative decay is independent from (M, R, S). Even when translation invariant they are not a conditional probability density function, they represent the functional dependency of the random spectral acceleration on the random variates, magnitude, distance and measurement error (Klügel, ENGEO 90, 186-192, 2007).

Step 4 - ???

M - magnitude; R - source distance; S - local soil conditions

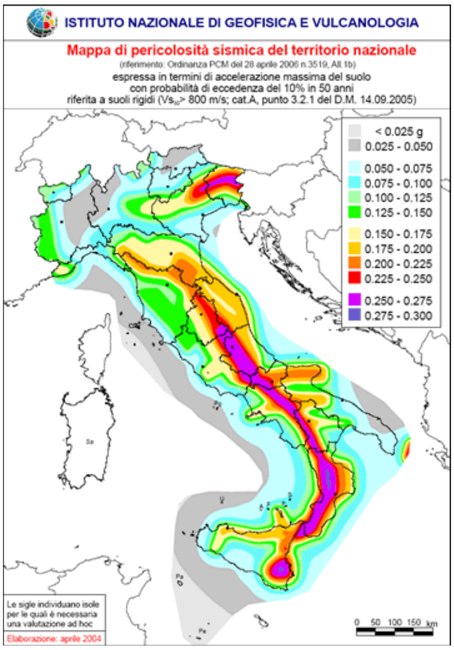

Probabilistic seismic hazard map of Italy expressed in terms of expected PGA (g) with a probability of exceedance of 10% in 50 years (return period 475 years). From the web page http://zonesismiche.mi.ingv.it/mappa_ps_apr04/italia.html

The new national hazard map and related seismic code is based on methodologies and related computer codes that are more than 20 years old and thus cannot accommodate the major recent steps forward made in Seismology.

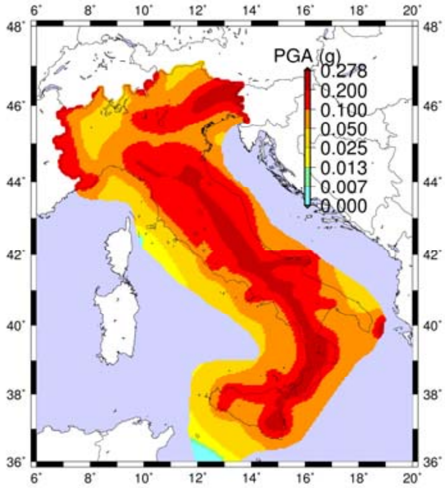

Probabilistic seismic hazard map of Italy expressed in terms of expected PGA (g) with a probability of exceedance of 10% in 50 years (return period 475 years). The map is drawn according to the estimations by Gruppo di Lavoro (2004), available at:

http://zonesismiche.mi.ingv.it/.

To facilitate the comparison, the colour palette is the same used for the neo-deterministic maps: each interval corresponds to one degree of intensity. The original map is available at: http://zonesismiche.mi.ingv.it/mappa_ps_apr04/italia.html

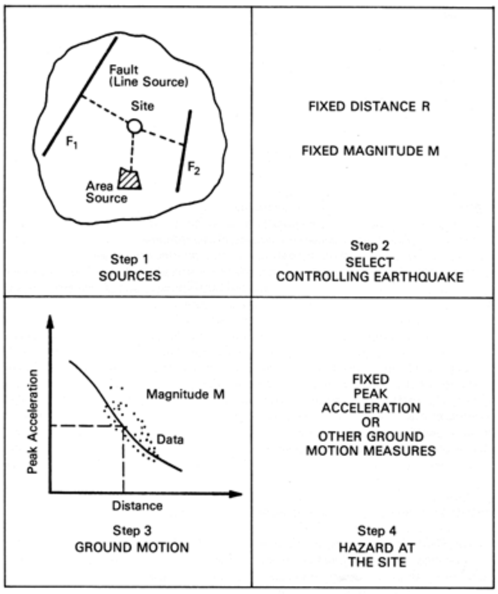

FIGURE 4.1 Basic steps of deterministic seismic hazard analysis (after TERA Corporation 1978).

Deterministic

Step 3 - Most of the attenuation relations usually are not translation invariant in the phase space (M, R, S), i.e. the relative decay is independent from (M, R, S). Even when translation invariant they are not a conditional probability density function, they represent the functional dependency of the random spectral acceleration on the random variates, magnitude, distance and measurement error (Klügel, ENGEO 90, 186-192, 2007).

M - magnitude; R - source distance; S - local soil conditions

- The attenuation relationships of the ground motion parameters can differ in the assumed functional form, the number and definition of independent variables, the data selection criteria, and the statistical treatment of the data.
- Attenuation relations, often emphatically called laws, assume the same propagation model for all the events, but such a hypothesis is not very realistic.

- The most frequently used attenuation relations of ground motion parameters, like PGA, PGV, have the form:

$$\log y = a + b\,M + c \log r_f + d\,D_f + e\,S \quad (1)$$

- where y is the ground motion parameter, a, b, c, d, e coefficients empirically determined, r_f and D_f are different measures of the distance from the source and S is a binary variable (0, 1) which depends on the soil type.

D_f is the closest distance from the intersection, with the free surface, of the fault plane or with its extension to the surface, for blind faults (the strike of the fault);

$$r_f^2 = D_f^2 + h_o^2$$

where h_o represents a reference depth. The value of h_o is different when dealing with PGA or PGV, and usually varies between 5 and 10 km for PGA and between 3 and 10 for PGV.

- The coefficients are determined empirically and turn out to be quite sensitive to the data set utilized.
- Usually regional data sets are statistically not significant, while the national or global data sets, even if statistically significant, they can represent very different seismotectonic styles that are not mixable. Quite often the coefficients are obtained in such a way that they turn out to be (almost) independent from magnitude, distance and soil type.

- If we consider the **relative decay** $R_y = y_{r_f}/y_{source}$, where r_f is the distance from the source and the suffix source indicates the values at the closest instrument to the source, typically D_{source} is about 2 km, we have

$$\log R_y = c(\log r_f - \log r_{source}) + d(D_f - D_{source}) \quad (2)$$

- i.e. R_y does not depend upon the magnitude (size of the event) and the kind of soil (local soil conditions).

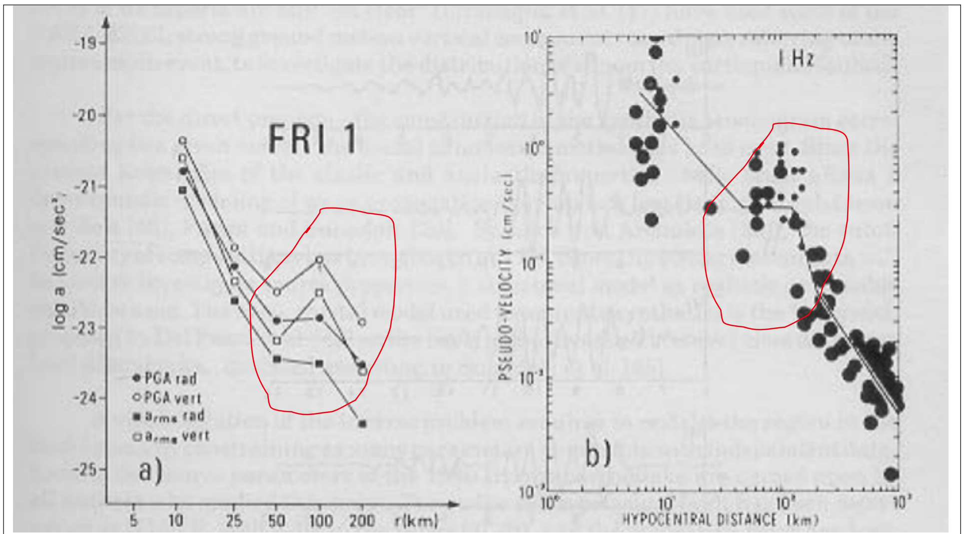

a) Theoretical attenuation relation showing the effect of critical reflection

b) Observed attenuation relations (Burger et al., 1987, BSSA)
While the elevated ground motion amplitudes in this distance range are usually not large enough by themselves to cause damage, they may produce damage if combined with the amplifying effects of soft soils.

Therefore empirical relations like (1) are not capable to capture relevant aspects of the phenomenon of space attenuation of peak values. This is not surprising since the difference between (2) and (1) indicates that (1) is not translation invariant, i.e. it has not a general physical meaning.

? GSHAP ?

Kobe (17.1.1995), Gujarat (26.1.2001), Boumerdes (21.5.2003) Bam (26.12.2003), E-Sichuan (12.5.2008) and Haiti (12.1.2010) earthquakes PGA(g)

	Expected with a probability of exceedence of 10% in 50 years (return period 475 years)	Observed
• Kobe	0.40-0.48	0.7-0.8
• Gujarat	0.16-0.24	0.5-0.6
• Boumerdes	0.08-0.16	0.3-0.4*
• Bam	0.16-0.24	0.7-0.8
• E-Sichuan	0.16-0.24	0.6->0.8
• Haiti	0.08-0.16	0.3-0.6*

*from I, if non linear effects (e.g. liquefaction) is considered the value may be smaller

Global Seismic Hazard Assessment Program (GSHAP) was launched in 1992 by the International Lithosphere Program (ILP) with the support of the International Council of Scientific Unions (ICSU), and endorsed as a demonstration program in the framework of the United Nations Interanational Decade for Natural Disaster Reduction (UN/IDNDR). GSHAP terminated in 1999.

Bilham (2009) supplies a list of potentially fatal flaws in our present day application of earthquake risk reduction. All can be ascribed to ignorance in one form or another. The first four are intrinsic to the methodology of earthquake risk assessment.
False Assumption #1. Seismic hazard maps or maps of seismic risk indicate the probability of future shaking intensity.
False Assumption #2. The most recent seismic hazard map is the most reliable available.
False Assumption #3. If sufficient funds and people are focussed on a local seismic risk problem, a reliable data base of historical data can be compiled to calculate probabilistic forecasts of future seismicity.
False Assumption #4 A global view of earthquake risk will improve our understanding of local seismic risk.
The remaining dozen items listed are issues that are rarely considered in risk estimation, but in the developing nations are responsible for current weaknesses in the implementation of safe housing.

Earthquake, Year, M*	Probability of exceedance 10% in 50 yrs (return period 475 yrs) PGA (g) (GSHAP)	Observed PGA (g)	Neo-DSHA PGA (g)
Kobe, Japan, 1995, M 7	0.40-0.48	0.7-0.8	
Gujarat, India, 2001, M 8	0.16-0.24	0.5-0.6	0.3-0.6
Boumerdes, Algeria, 2003, M 6-3/4	0.08-0.16	0.3-0.4	0.4-0.6
Bam, Iran, 2003, M 6-1/2	0.16-0.24	0.7-0.8	
E-Sichuan, China, 2008, M 8	0.16-0.24	0.6->0.8	
Haiti, 2010, M 7	0.08-0.16	0.3-0.6	
			DSHA PGA (g)
Landers, California, 1992, M 7-1/4	<0.2	**	0.6
Northridge, California, 1994, M 6-3/4	<0.4	**	0.6

**No records in the near-field but observed effects indicated comparable DSHA and PGAs but much higher than probabilistic PGAs (Mualchin, 1996 - ENGEO, 42, 217-222).
EARTHQUAKE - Hazard, Risk, and Strong Ground Motion. Ed: Y.T. Chen, G.F. Panza and Z.L. Wu, Seismological Press, 323-349, 2004.

NEO-DETERMINISTIC

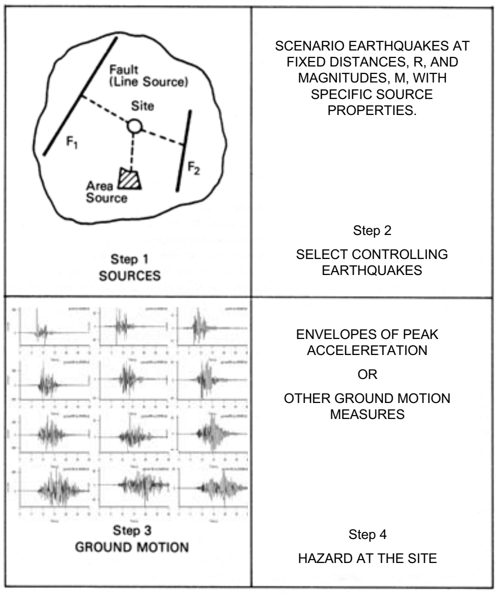

New approach based on synthetic signals computation

No need of attenuation relations

Neo-deterministic procedure at national scale

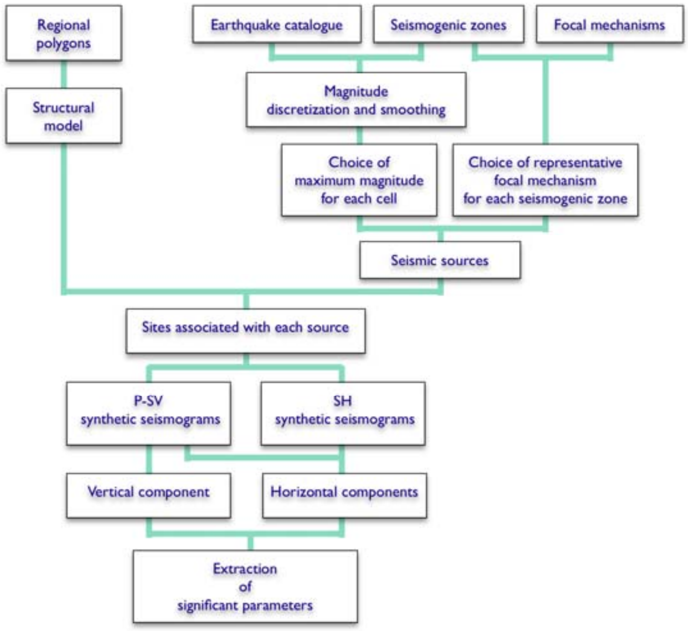

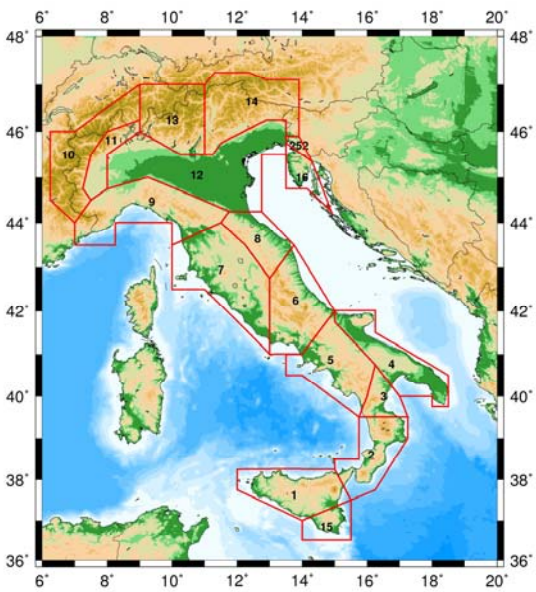

Regional polygons defined in the framework of GNDT activities, associated with average structural models (Panza et al., Advances in Geophysics, 43, 1-95, 2001).

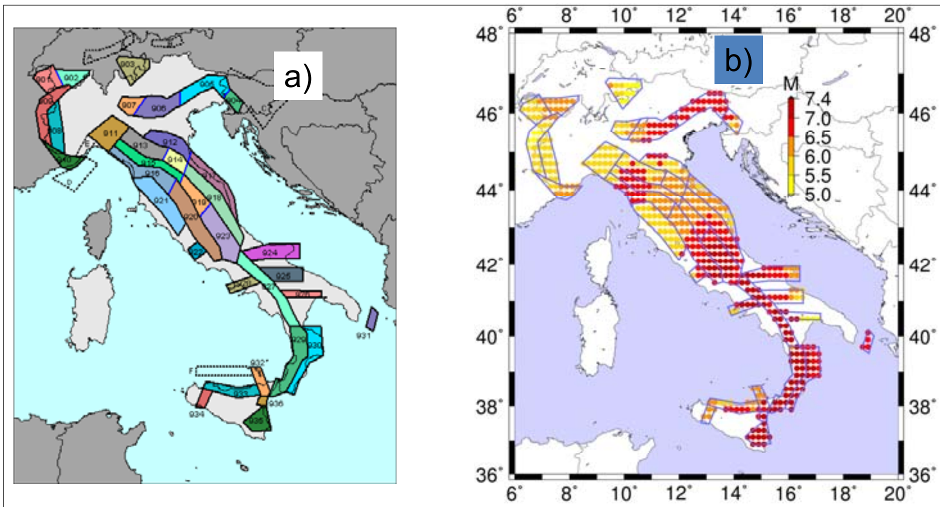

a) Seismogenic zones ZS9 (Meletti and Valensise, 2004).

b) Seismic Sources, within the seismogenic zones ZS9 (Meletti and Valensise, 2004), used for the generation of synthetic seismograms. Magnitude from discretization and smoothing of seismicity in the CPTI04 catalogue (Gasperini et al., 2004).

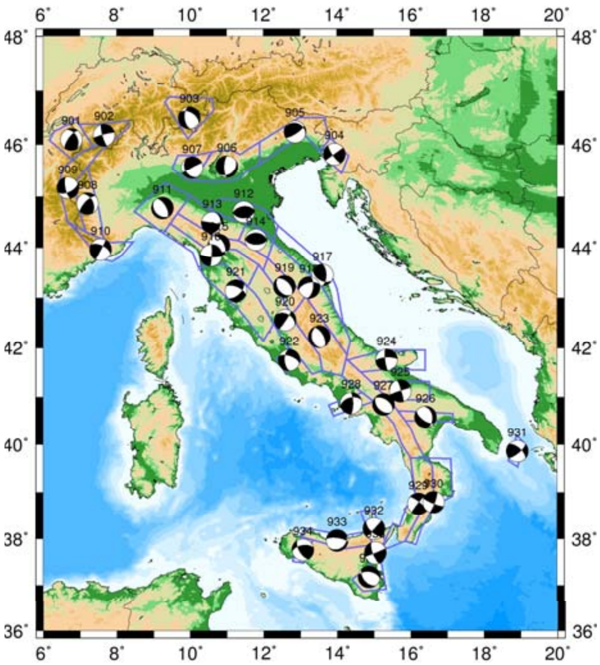

Focal mechanisms associated with the seismogenic zones ZS9 (Meletti and Valensise, 2004).

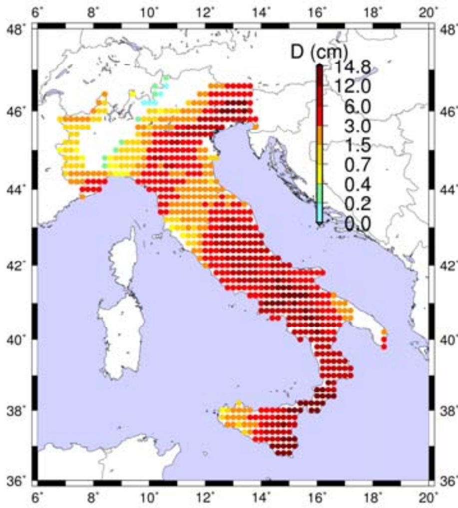

Map of peak displacements

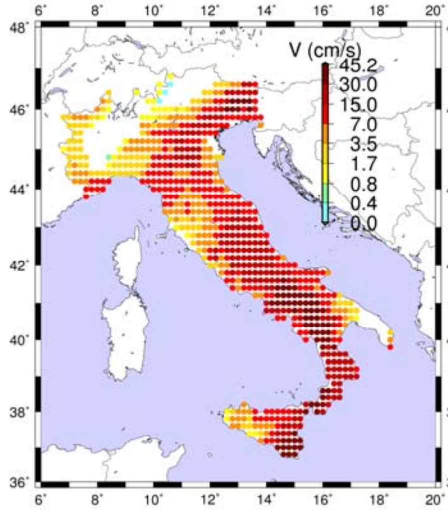

Map of peak velocities

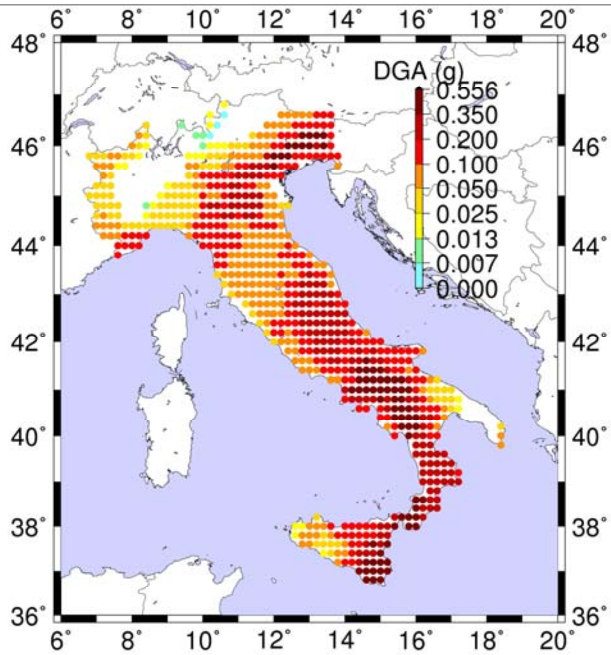

Map of DGA.

NDSHA has been applied in many countries, like:

China (Ding Z.; Chen -Y.T)

India (Parvez I.; Mohanty W.)

Viet Nam (Cao D.T.)

Egypt (El-Sayed A.)

Algeria (Benouar D.; Harbi A.)

Bulgaria (Paskaleva I.; Kouteva M.)

Romania (Radulian M.; Marmureanu G.; Cioflan C.)

More info in Episodes, 2002, 25, 160-184.

Stability tests show that the seismicity level, defined by earthquakes with M≥5.0, increased in the last 500 years with respect to that of the period [1000,1499]. A similar conclusion has been obtained by Vorobieva and Panza (Pure Appl. Geophys., 141, 25-41,1993).

This observation suggests that the available information from past events **may well not be representative of future earthquakes and that the use of independent indicators of the seismogenic potential of a given area is needed**.

The flexibility of the neo-deterministic method permits, among others, to incorporate the additional information about the possible location of strong earthquakes provided by the morphostructural analysis.
This is impossible with PSHA!

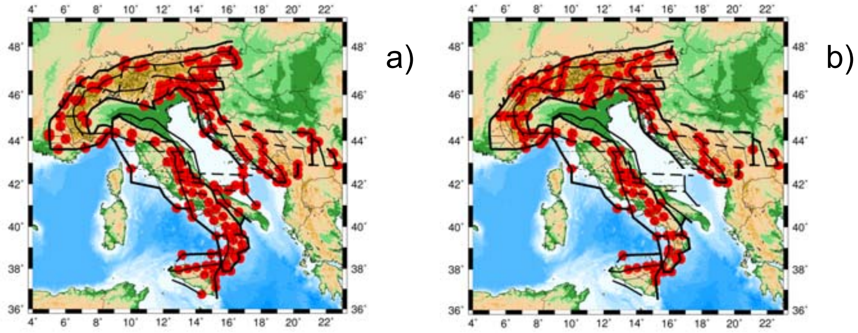

Morphostructural map of Italy and surrounding regions (Gorshkov et al., JSEE, 4, 1-24, 2002; Boll. Soc. Geol. It., 123, 3-18, 2004). Lines with different thicknesses indicate morphostructural lineaments of different rank: thick lines first order lineaments, medium lines to second order lineaments and thin lines to third order lineaments. Longitudinal lineaments are marked by continuous lines and transversal lineaments by dashed lines. Circles represent the nodes prone to earthquakes with magnitude a) M≥6.0 and b) M≥6.5, respectively.

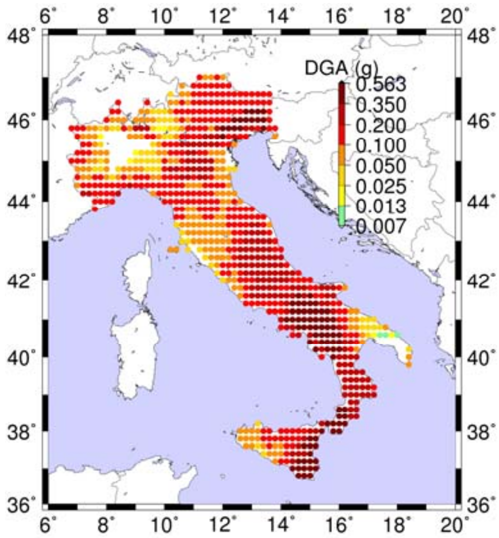

DGA map computed using **both the seismogenic zones** (Meletti and Valensise, 2004) and **the seismogenic nodes** (Gorshkov et al., 2002, 2004).

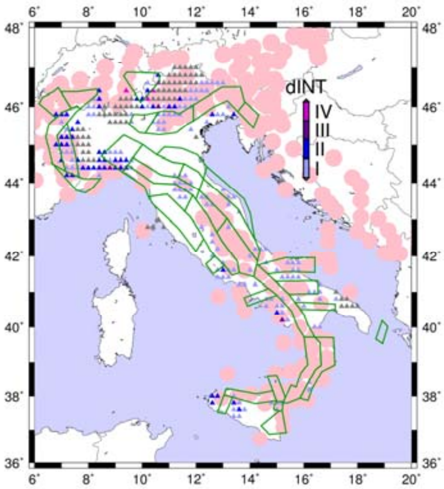

Differences in intensity between the DGA maps computed **with** (DGA_{nodes}) and **without** seismogenic nodes. The upward triangles indicate a positive difference, while the downward triangles indicate a negative difference. The grey triangles are the points for which no value is given when not considering seismogenic nodes. The seismogenic zones ZS9 (polygons, Meletti and Valensise, 2004) and the distribution of seismogenic nodes for both M≥6.0 and M≥6.5 (filled circles, Gorshkov et al., 2002, 2004) are shown as well.

The stability analysis, made considering the time intervals [1000,1499] and [1500,1999], has been repeated **introducing the seismogenic nodes** into the neo-deterministic computation.

As expected, the differences are smaller than when seismogenic nodes are not considered, since the contribution of the seismogenic nodes somehow supplies the seismicity missing due to the limited (500 years) time windows considered in the stability experiment.

MACROSEISMIC INTENSITY

Peak value (I-1)/Peak value (I)=2

ING (Boschi et al., 1995a)

Intensity	D (cm)	V (cm/s)	DGA (g)
V	0.2 - 0.4	0.4 - 0.8	0.007 - 0.013
VI	0.4 - 0.7	0.8 - 1.7	0.013 - 0.025
VII	0.7 - 1.5	1.7 - 3.5	0.025 - 0.05
VIII	1.5 - 3.0	3.5 - 7.0	0.05 - 0.10
IX	3.0 - 6.0	7.0 - 15.0	0.10 - 0.20
X	6.0 - 12.0	15.0 - 30.0	0.20 - 0.35
XI	12.0 - 24.0	30.0 - 62.0	0.35 - 0.70

Cancani in 1904 modified Mercalli scale with the declared purpose to obtain the 2 factor.

ISG (Molin et al., 1996)

Intensity	D (cm)	V (cm/s)	DGA (g)
VI	0.5 - 1.0	0.8 - 1.7	0.01 - 0.025
VII	1.0 - 2.0	1.7 - 4.0	0.025 - 0.05
VIII	2.0 - 4.0	4.0 - 9.0	0.05 - 0.10
IX	4.0 - 8.0	9.0 - 20.0	0.10 - 0.20
X	8.0 - 17.0	20.0 - 46.0	0.20 - 0.50

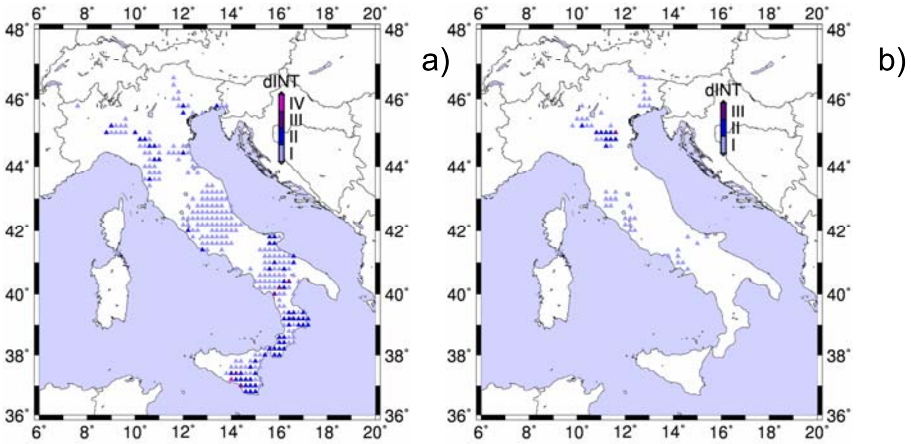

Differences in intensity between the NDSHA map computed considering the whole catalogue and the map computed including the seismogenic nodes (Gorshkov et al., 2002, 2004), for the period a) [1000,1499], b) [1500,1999]. The upward triangles indicate a positive difference, while the downward triangles indicate a negative difference.

DGA and PGA, parameters currently used in PSHA and NDSHA maps, respectively, although both expressed in units of g, represent different physical quantities. **PGA** is the horizontal peak ground acceleration with 10% probability of being exceeded in 50 years. This quantity is obtained treating probabilistically both the available information about the seismicity observed within each Seismogenic Zone and the propagation of seismic waves (attenuation relations).
DGA is the horizontal acceleration anchoring the elastic response spectrum at the period T=0 s, computed from the response spectrum obtained through the modelling of the ground motion caused by the strongest earthquakes observed in each cell falling in the Seismogenic Zones.

DGA is comparable to PGA, since an infinitely rigid structure (i.e. a structure having a natural period of 0 s) moves exactly like the ground (i.e. the maximum acceleration of the structure is the same as that of the ground, which is the PGA). This is why PGA has been used over the years to provide a convenient anchor point for the design spectra specified by various regulatory agencies. Moreover, DGA is practically equivalent to EPA (Effective Peak Acceleration), which is defined as the average of the maximum ordinates of elastic acceleration response spectra within the period range from 0.1 to 0.5 seconds, divided by a standard factor of 2.5, for the 5% damping (Panza et al., NEA/CSNI/R 18, 241-266, 2003).

Since the available earthquake catalogue (CPTI04 - Gruppo di Lavoro CPTI, 2004) appears to be complete for M≥5, therefore sufficient for DGA estimation, during at least 1000 years (Vorobieva and Panza, Pure Appl. Geophys., 141, 25-41,1993), it can be considered representative of a return period of about 500 years (sampling theorem); this also on account of the described stability tests, where we have shown that the analysis cannot be limited to 500 years of catalogue. Therefore the comparison between DGA and PGA (return period 475 years) is justified. **This comparison is possible only in Italy thanks to the uniqueness of the length of its earthquake catalogue.**

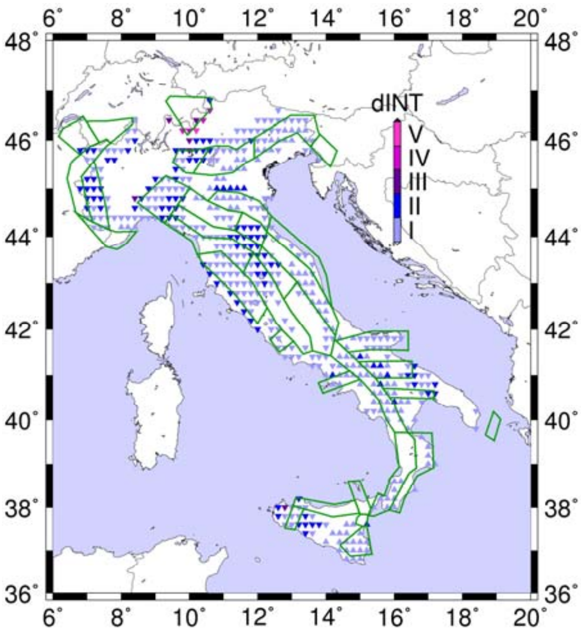

Differences, in terms of macroseismic intensity, between NDSHA and PSHA maps. The upward triangles indicate a positive difference, while the downward triangles indicate a negative one. The seismogenic zones ZS9 (Meletti and Valensise, 2004) are shown as well.

The points where the NDSHA is giving larger values than the PSHA are located in correspondence of the strongest observed earthquakes (e.g. Friuli, Central-Southern Apennines, Calabrian Arc and eastern part of Sicily), as it can be expected, since seismicity has been smoothed within the seismogenic zones. This fact supports the idea that PSHA underestimates the hazard in high-seismicity areas. As a natural consequence of its smoothing property PSHA overestimates hazard in low-seismicity areas.

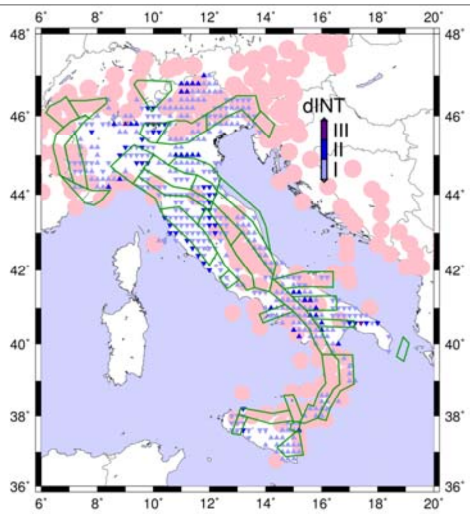

Differences in intensity between the NDSHA (**taking into account seismogenic nodes**) and PSHA maps. The seismogenic zones ZS9 (Meletti and Valensise, 2004) and the distribution of seismogenic nodes for both M≥6.0 and M≥6.5 (filled circles, Gorshkov et al., 2002, 2004) are shown as well.

The differences, in the common points, between the NDSHA map and the PSHA one have been computed also with respect to the map in which the seismogenic nodes are included in the NDSHA computation. **The PSHA turns out to be lower than that provided by NDSHA not only in correspondence of the largest observed earthquakes but also in correspondence of the areas identified as prone to large earthquakes, where a strong earthquake has not yet occurred. In low-seismicity areas, PSHA supplies values that are higher compared with those given by NDSHA; this is a natural consequence of the smoothing property of PSHA.**

The comparison of the seismic hazard maps produced for Italy by the PSHA and NDSHA approaches shows that, as a rule, NDSHA provides values larger than those given by the PSHA in high-seismicity areas and in areas identified as prone to large earthquakes, but where no strong earthquake has been recorded in the last 1000 years.

COMPARISON PSHA-NDSHA

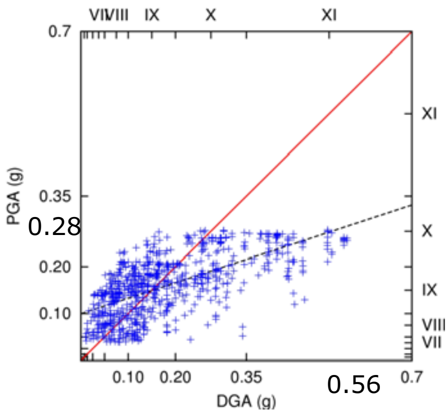

10% Probability of exceedance
in 50 years
T = 475 years

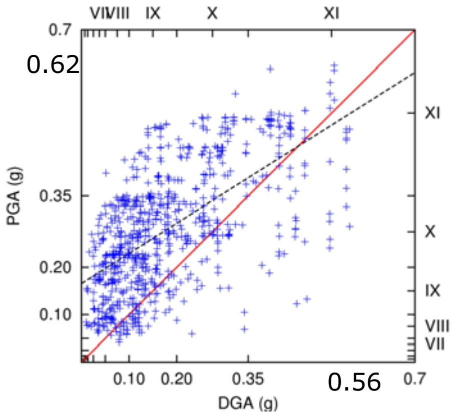

2% Probability of exceedance
in 50 years T = 2475 years

Conclusions

The limited historical seismic record makes PSHA inadequate for the effective protection from seismic hazard, in particular of NPP from seismic hazard.

A viable alternative is represented by the neo-deterministic approach (NDSHA), that requires only the classification of earthquakes into exceptional (catastrophic), rare (disastrous), sporadic (very strong), occasional (strong) and frequent.

Conclusions

Therefore NDSHA may provide an upper bound for the ground motion levels to be expected, more appropriate than probabilities of exceedance in view of the long time scales required for the protection of NPP.

NDSHA naturally supplies realistic and reliable estimates of ground displacement readily applicable to seismic isolation techniques.

MERCEA'08
2008 Seismic Engineering International Conference
commemorating the 1908 Messina and Reggio Calabria Earthquake

Low-Frequency Seismic Ground Motion at the Pier Positions of the Planned Messina Straits Bridge for a Realistic Earthquake Scenario

Authors: A.A. Gusev[a,b], V. Pavlov[b], F.Romanelli[c], and G.Panza[c,d]

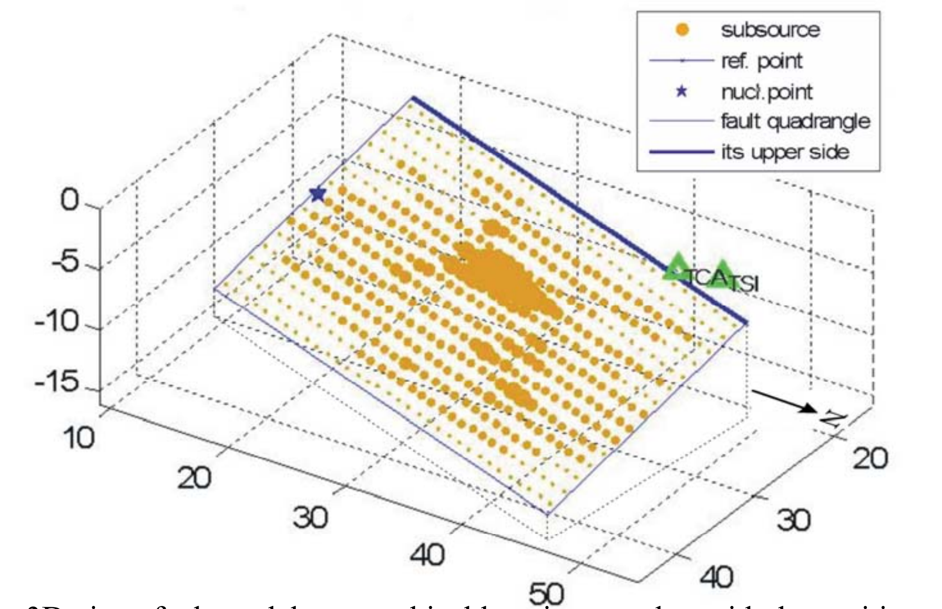

3D view: fault model geographical location together with the position of the two piers: Torre Calabria, TCA and Torre Sicilia, TSI. Star is the rupture nucleation point.

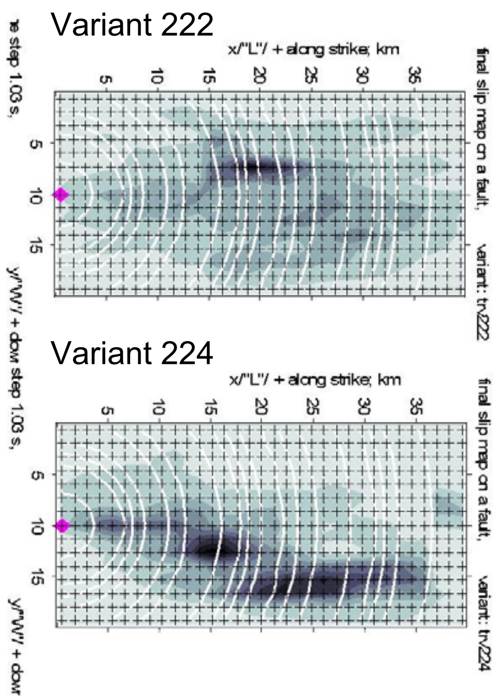

Slip or $M_o(x,y)$ distribution by levels of grey. Diamond is the nucleation point, and white contours are rupture front positions every 1.03 s

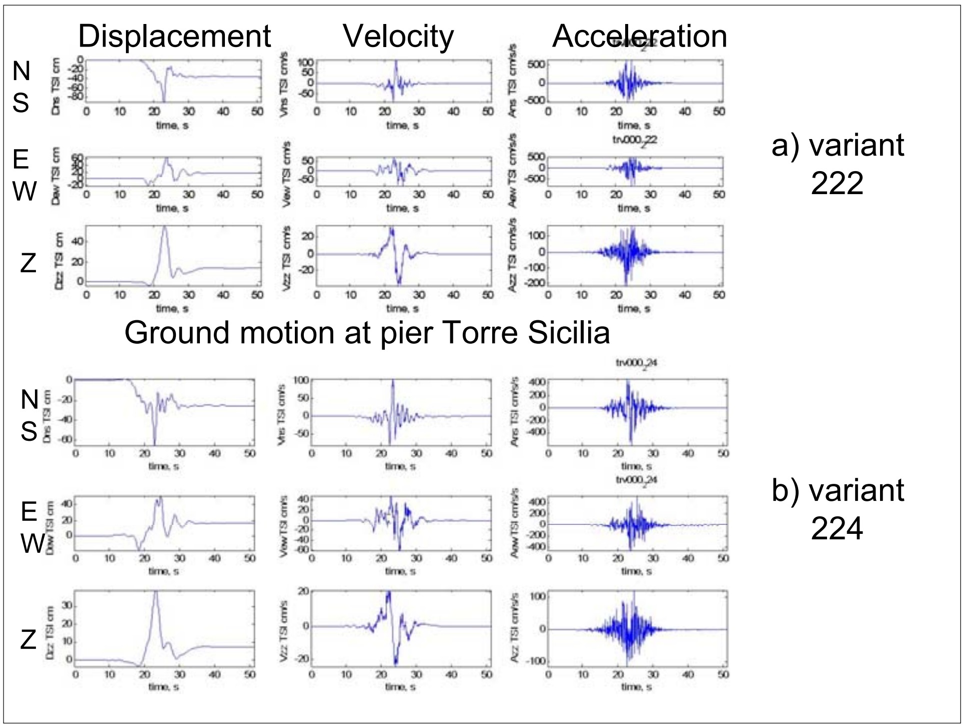
Displacement
Velocity
Acceleration
N
S
E
W
Z
a) variant
222
Ground motion at pier Torre Sicilia
b) variant
224

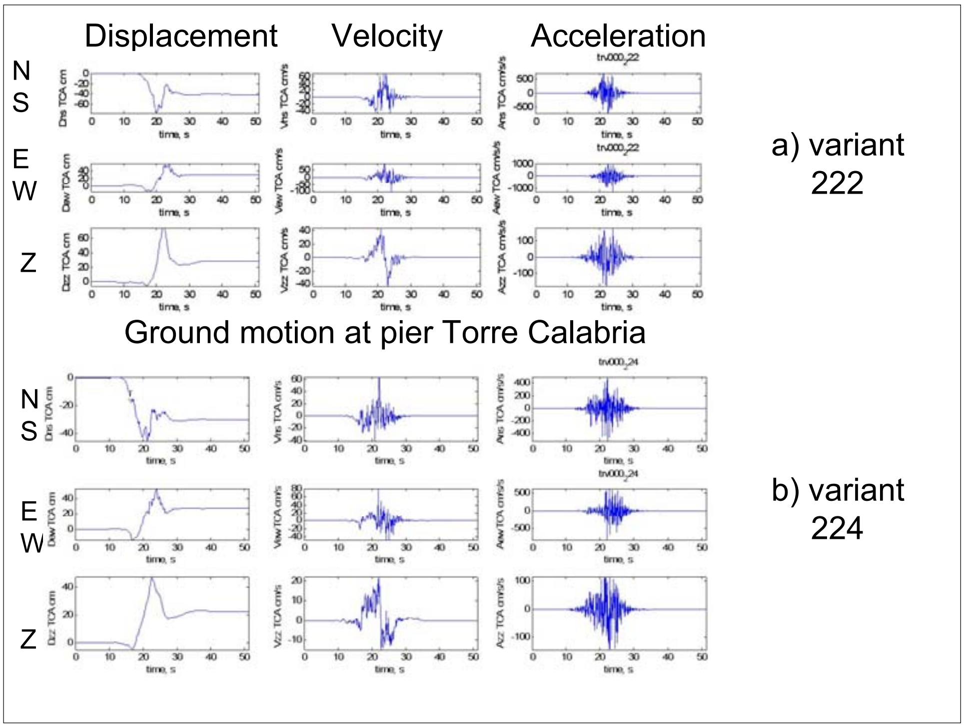
Displacement
Velocity
Acceleration
N
S
E
W
Z
a) variant
222
Ground motion at pier Torre Calabria
b) variant
224

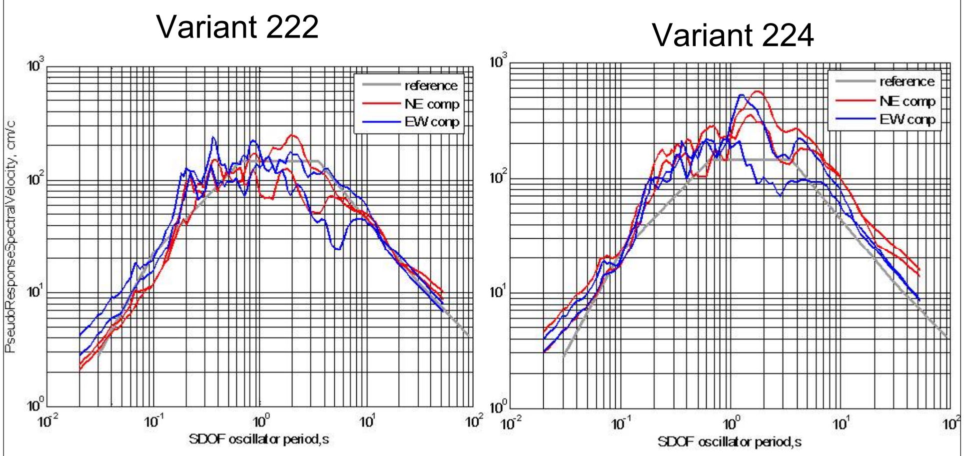

PRV (response velocity spectra) for horizontal components, both piers on one plot. Variant 224 exceeds significantly the reference spectrum (SM-PRV), proposed by Stretto di Messina (2004).

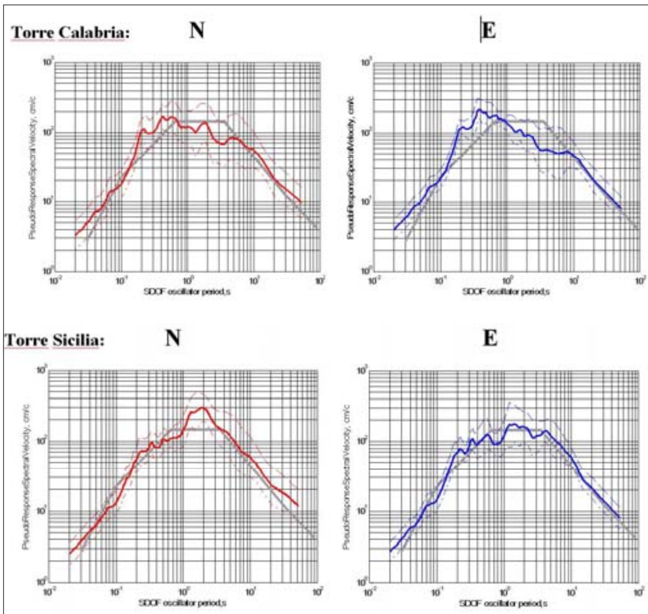

Median, and +/- 1 r.m.s. deviation band, for response velocity spectra at the two piers

Median PRV slightly above the SM-PRV for T> 4 s. For 1<*T*<4 s, the levels of N and E median components differ: E is close to the SM-PRV spectrum, N (oriented roughly along fault slip) is significantly larger, up to 2 times at *T*=2 s. The r.m.s. deviation of individual spectra corresponds to the variation of +65% / -40% with respect to the median. If a 84% upper quantile (median+1σ) motion is selected as **a safe upper limit,** it must be positioned at 1.65 times above our median spectrum**, or from 1.8 to 2.8 times above the SM-PRV spectrum.**

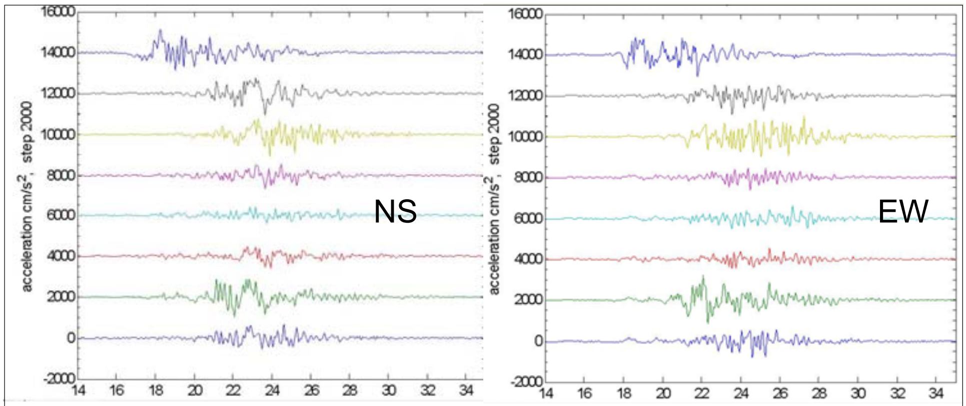

Examples of the considerable variability of the accelerograms in the individual simulations. Eight sample functions of the ground acceleration at Torre Sicilia for the horizontal components. Vertical interval between zero-lines of traces is 2000 cm/s^2 . The first trace is for the less usual source sample function, when a large asperity happened to coincide with the spot with the highest permitted propagation velocity

CONCLUSIONS

We compare a set of response horizontal velocity spectra (PRV) obtained from our calculations with a reference PRV that is considered as a reasonable upper bound for the possible ground motion near the piers. Our results suggest that the seismic ground motion under Torre Sicilia dominates that under Torre Calabria and that the median PRV is **generally above the reference one**, about 1.1-1.3 times for T>4 s, and up to 2 times for 1<T≤4 s.

CONCLUSIONS

The efficiency of the computer codes, accounting for the statistical variation in individual spectra, makes it easy the prediction of earthquake ground motion for any suite of plausible source models. As an example, one can use a 84% upper quantile of the distribution of the spectral ordinates generated from a sufficiently large set of simulated accelerograms.

CONCLUSIONS

The use of advanced fault and medium models, accounting also for the natural scatter of individual PRV spectra due to events with the same gross source parameters, provides a sound basis for the deterministic engineering estimates of future earthquake ground motion.

Pure and Applied Geophysics
Topical volume
2010

Advanced Seismic Hazard Assessment

Editors: *G.F. Panza (Italy), K. Irikura (Japan), M. Kouteva (Bulgaria), A. Peresan (Italy), Z. Wang (USA), R. Saragoni (Chile)*

ASI Pilot Project - SISMA
"Seismic Information System for Monitoring and Alert"

Development of a system, based on the neo-deterministic approach for the estimation of seismic ground motion, integrating the space and time dependent information provided by real-time monitoring of seismic flow and EO data analysis, through geophysical forward modeling.

agenzia spaziale italiana

DST

University of Milano

Politecnico di Milano

galileian PLUS

About convolutive/deconvolutive methods

In the far field (and in the point source approximation, i.e. in the simplest possible case) the displacement (the seismogram) is:

$u_k(t)=M_{ij}(t)*G_{ki,j}(t)$

k, i and j are indices and ,j means derivative, * means convolution, G is the Green's function and M_{ij} are moment tensor rate functions.

If the M_{ij} are considered to be independent in the description of the source, the above equation is linear (it corresponds to a mechanism generally varying with time).

However, if we constrain the independence of M_{ij} and ask for a constant mechanism (even unconstrained one, i.e. the full moment tensor), i.e. if we impose the constraint $M_{ij}(t)=M_{ij}.m(t)$ the problem becomes non-linear because of the product on the right-hand side of:

$u_k(t)=M_{ij}.m(t)*G_{ki,j}(t)$

both M_{ij} and m(t) are model parameters controlling source properties.

Thus, the problem in the time domain is non-linear even without the DC constraint (the DC constraint is an additional non-linearity here).

In the frequency domain it may seem simpler because the above convolution is converted to pure multiplication:

$$u_k(\omega)=M_{ij}(\omega)\cdot G_{ki,j}(\omega)$$

and the equation is solved for each frequency separately. Within linearity we get $M_{ij}(\omega)$ but to split the source time function and the mechanism again a non-linear constraint is needed, so the advantage of the frequency domain is fictious only.

The non-linearity consisting in the DC constraint is an additional one. It is based on the fact that the DC constraint needs non-linear combination of the components of the moment tensor, namely zero value of its determinant (contrary to the deviatoric constraint which needs zero trace of the moment tensor which is a linear combination).

A>0

B>0

(A+B)/(A-B)=x

A+B=x(A-B)

If A=B=1 we have

2=0

References

Sileny, J. and Panza, G.F. (1991). Inversion of seismograms to determine simultaneously the moment tensor components and source time function for a point source buried in a horizontally layered medium. Studia Geophysica et Geodaetica, 35, 166-183.

Sileny, J., Panza, G.F. and Campus, P. (1992). Waveform inversion for point source moment tensor retrieval with variable hypocentral depth and structural model. Geophys. J. Int., 109, 259-274.

Paskaleva, I., Dimova, S., Panza, G.F. and Vaccari, F., (2007). An Earthquake scenario for the microzonation of Sofia and the vulnerability of structures designed by use of the Eurocodes. Soil Dynamics and Earthquake Engineering, 27, pp. 1028-1041.

The use of synthetic seismograms is imposed by the necessity to bypass the problem arising from the fact that so called site effects, are rather a wishful thinking than a physical reality and the local response is strongly influenced by the source, as shown in what follows.

•**H/V** is the spectral ratio between horizontal and vertical components of motion.

•**RSR** is the ratio between the response spectra amplitudes (5% damping) obtained with the local and the bedrock structures

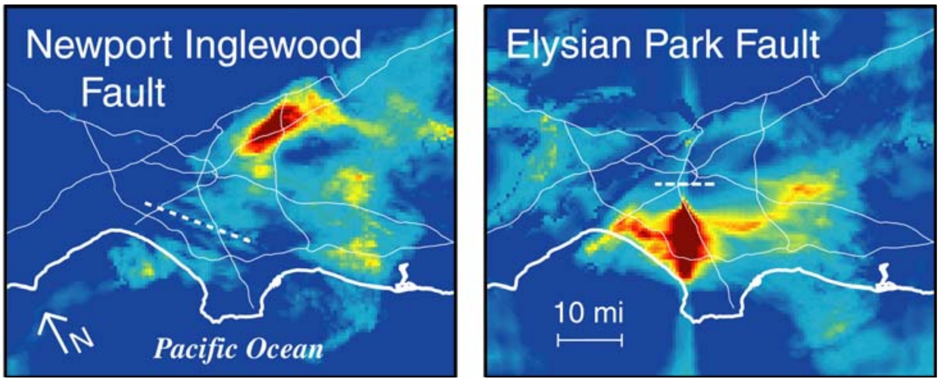

These images of the Los Angeles Basin show "hotspots" predicted from computer simulations of an earthquake on the Elysian Park Fault and an earthquake on the Newport-Inglewood Fault (represented by the white dashed lines). What is shown is **not** how much shaking was experienced at a particular site but rather how much more or less shaking (highest levels are shown in red) a site receives **relative to what is expected** from only the magnitude of the earthquake and the site's distance from the fault. These images consider only part of the total shaking (long-period motions) and were calculated by using a simplified geologic structure. (Data for images courtesy of Kim Olsen, University of California, Santa Barbara, SCEC Phase III report)

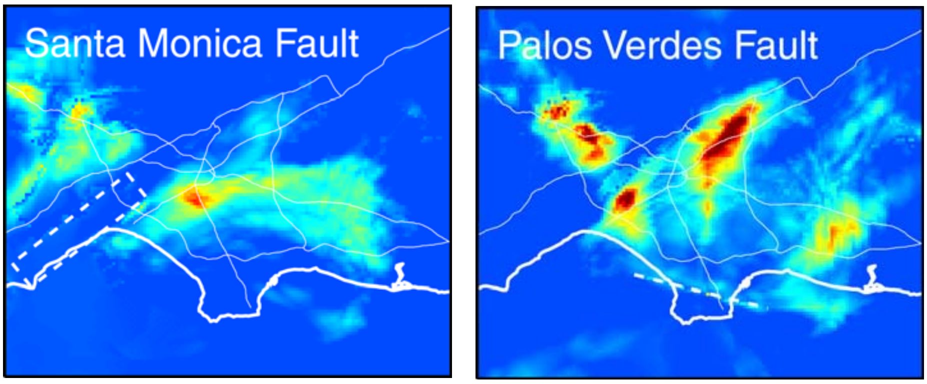

"hotspots" predicted from computer simulations of an earthquake on the Santa Monica Fault and an earthquake on the Palos Verdes Fault (represented by the white dashed lines). SCEC Phase III report, Field, 2000, BSSA, see also http://www.scec.org/phase3/

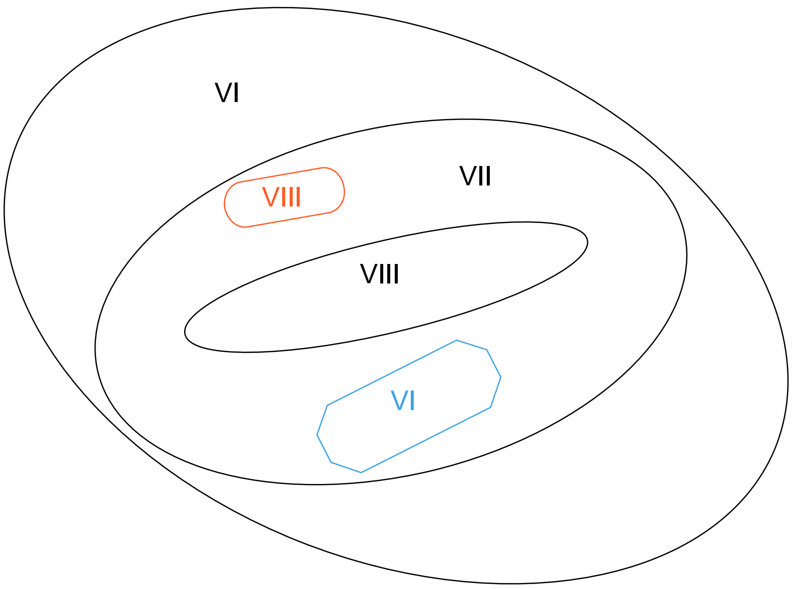

Schematic representation of multi-connected isoseismals

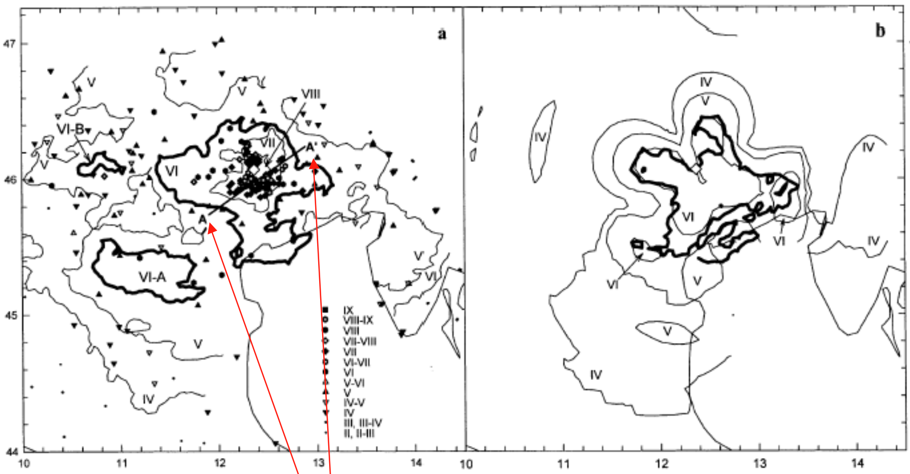

Alpago earthquake (18.10.1936, M_L=5.8): MCS Intensity data (*point-like symbols*) and isolines defined with polinomial filtering; segment (A, A′) separates the zone with I≥VI on mountain from that on plain. Areas VI-A e VI-B are local effects?

(b) isolines of the synthetic a_p-field (*thin line*) and reconstruction of the theoretical I_a=VI isoline (*bold line*) using the original observation points and the polynomial filtering technique (Molchan et al., 2002, PAGEOPH, 159).

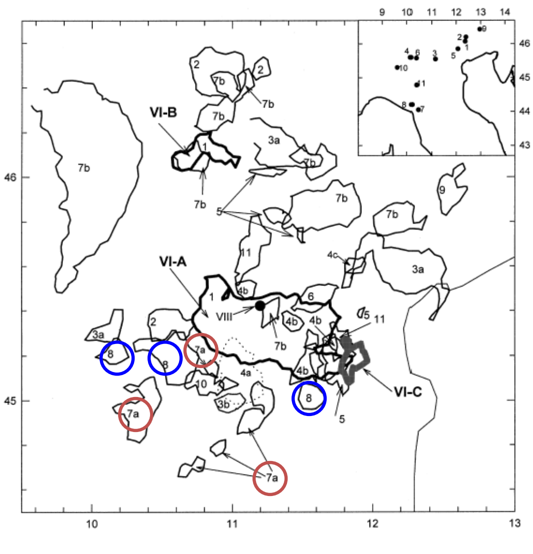

1) 18.10.1936, Alpago, V+1 (*think line*; VI-A, VI-B), area VI-C is an alternative to the area VI-A due to instability of the the polynomial.

2) 29.06.1873, Bellunese, V+1 (2).

3) 7.06.1891, Veronese, IV+1 (3a), V+1 (3b).

4) 27.11.1894, Franciacorta, IV-1 (4a, *dotted line*), III+1 (4b), II+1 (4c).

5) 4.03.1900, Valdobbiadene, IV+1 (5).

6) 30.10.1901, Salo, IV+1 (6).

7) 27.10.1914, Garfagnana, V+1 (7a), IV+1 (7b).

8) 7.09.1920, Garfagnana, IV+1 (8).

9) 12.12.1924, Carnia, IV+1 (9).

10) 15.05.1951, Lodigiano, V+1 (10).

11) 15.07.1971, Parmense, IV+1 (11).

Secondary parts (*thin line*) of the multi-connected isoseismals for the 11 earthquakes in the zone of Alpago earthquake.

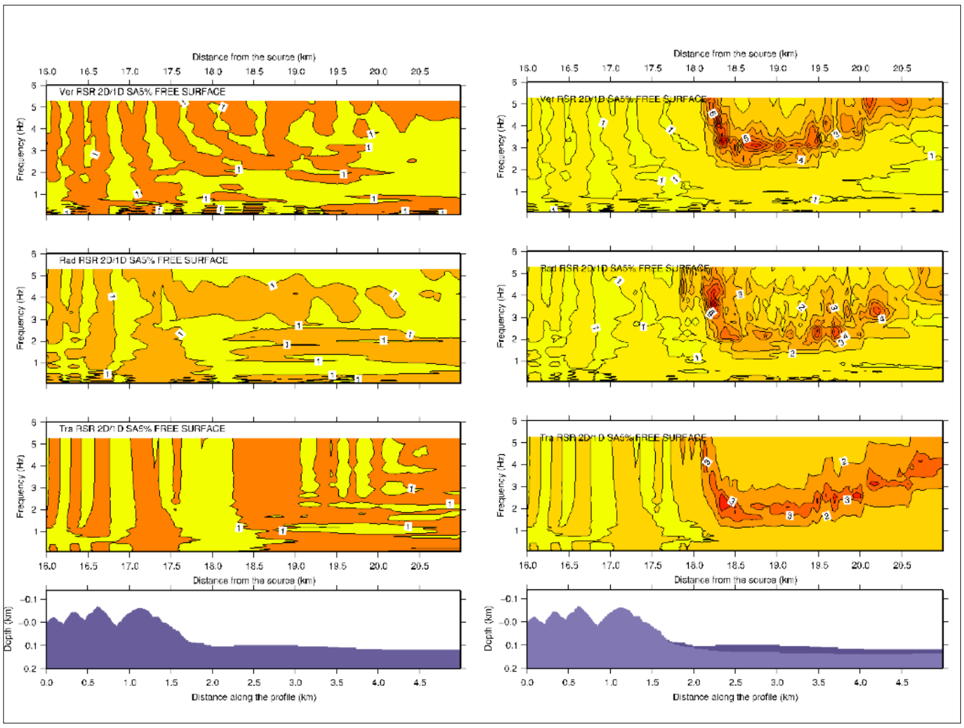

Thanks to **Mentors** and Co-workers:

Leon Knopoff

Volodya Keilis-Borok*

Yuntai Chen

Luis Decanini

Marian Herak

ImtyiazParvez

Mircea Radulian

Ding Zhifeng

*Alexander Gusev**

*Volodya Kossobokov**

*Igor Kuznetzov**

*Antonella Peresan**

*Fabio Romanelli**

*Franco Vaccari**

Elisa Zuccolo

**SAND/ICTP*